

# ASPECT RATIO EFFECTS IN FLOATATION SYSTEMS

M.J. DAVIES

AND

D.H. WOOD

RESEARCH & TECHNOLOGY CENTRE

JOHN LYSAGHT (AUST.) LTD.

PORT KEMBLA, NSW, 2505 AUSTRALIA

DEPT. OF MECHANICAL ENGINEERING

UNIVERSITY OF NEWCASTLE

N.S.W. 2308 AUSTRALIA

**SUMMARY** A study of aspect ratio effects in floatation systems is described. The essential component of such a system is a two jet nozzle which produces a force that decreases as the inverse of distance from the nozzle. At sufficiently low aspect ratios there is a range of floatation heights over which the force increases with distance from the nozzle. The aspect ratio has little effect on the transition from laminar to turbulent flow close to the jet exit and so does not cause the "feedback" that can occur in some impinging free shear layers. It is argued that the main effect of low aspect ratio is to allow a form of "communication" between the two jets over their entire length. If this communication is weakened by installing vortex generators at the exit of each jet to destroy any spanwise coherence of the jets, the resulting force becomes qualitatively similar to that in an "infinite" nozzle.

## 1 INTRODUCTION

Modern floatation ovens are used to dry and cure continuous thin metal strip that has been simultaneously painted or coated on both sides. The continuous strip passes through a series of ovens containing floatation nozzles arranged in pairs above and below the strip; only one half of the upper nozzle is shown in Figure 1. The upper and lower nozzles are identical and each nozzle is symmetric about the centre-line. Each nozzle produces a force on the strip that decreases roughly as the inverse of the distance from the nozzle, so that a system of opposing floatation nozzles can float a range of strip of varying thickness and density. A floatation nozzle is the two-dimensional analogue of a hovercraft, and the basic aerodynamics has been studied by Davies & Wood (1983; hereinafter referred to as DW), who considered only an "infinite" nozzle. In practice, a nozzle will have a finite aspect ratio, AR, defined as the ratio of the nozzle span,  $w$ , (out of the page in Figure 1) to  $b$ , the distance of the jet exit to the nozzle centre-line. The finite aspect ratio, which can significantly affect the operation of the nozzle, has no counterpart in hovercraft aerodynamics. In this paper we consider some of the effects of finite aspect ratio.

The simplest form of the theory assumes that the pressure inside the air cushion is uniform and the inviscid, thin jet remains at constant thickness,  $t$ , and velocity, while following a path that is tangential to both the direction of the slot at exit and the impingement surface. It is easy to show (DW) that for a jet inclined at an angle  $\theta$ , the gauge cushion pressure,  $P_c$ , is given by

$$J(1+\cos\theta) = P_c h \quad (1)$$

where  $J$  is the momentum flux per unit length of jet and  $h$  is the floatation height. The effect on the lift of jet inclination is conveniently described by defining  $A_t$ , the theoretical coefficient of ground effect, as the ratio of the lift per unit width ( $2P_c b + 2J\sin\theta$ ) to the force generated by a single vertical jet having the same momentum flux as the inclined jets ( $2J$ ). Using equation (1), the ratio is

$$A_t = b(1+\cos\theta)/h + \sin\theta \quad (2)$$

In general,  $P_c$  is usually small, but it acts over a large area resulting in a significant contribution to the lift. We will show later that  $A_t$  can have values very much larger than unity.

The analysis of DW was stimulated by the amazing success of the simplified inviscid analysis when compared to the experimental data of Jaumotte and Kiedrzyński (1964). DW showed that equations (1) and (2) are approximate solutions to the Reynolds-averaged Navier-Stokes equations for the flow. In other words, equations (1) and (2) are first order approximations to the real flow behaviour. They are independent of the mean velocity profile in the jet, whose thickness need not remain constant, although the jet must obey the classical "boundary layer" approximation. The only significant restriction is that the radius of curvature of the flow path must remain nearly constant.

We tested the adequacy of equation (2) at the centre-line of the two nozzle boxes, the first with a much smaller aspect ratio than that in an actual floatation oven, and the second with a comparable aspect ratio. Even if equation (2) applies at the centre-line there is no guarantee that it holds for all  $z$  (out of the page in Figure 1). We show that the lift is indeed  $z$ -dependent in the second nozzle box, and then concentrate on the more pronounced aspect ratio effects shown by the first nozzle box.

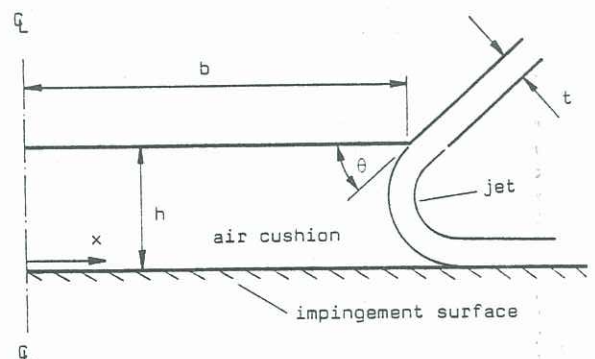


Figure 1 Half-sectional view of upper floatation nozzle.

## 2 EXPERIMENTAL DETAILS

Two nozzle boxes, denoted by NB1 and NB2, were tested. The span of NB1 was limited by the span of the wind tunnel available for the initial measurements. Subsequently, a new wind tunnel was built and NB2 was tested. The dimensions of both boxes are given in Table 1; note that both are of 3/4 scale in the x-direction. The jets emerged at a nominal  $\Theta$  of  $30^\circ$ .

In an attempt to simulate true two-dimensional behaviour, end plates were installed on each nozzle box to block any flow at the edges in the z-direction and force all the air to exit in the x-direction.

For both NB1 and NB2, the lift was obtained using a flat plate with about twenty 1 mm pressure tappings. The pressures for NB1 were measured manually using a Betz projection manometer. An automated data collection system was used for the tests on NB2. The tappings were connected via a 24-port Scanivalve to a Furness FC001 pressure transducer. The Scanivalve was controlled by a HP85 desk top computer through a specially built interface. The transducer output voltages were recorded by a HP3479A data logger.

Mean velocity measurements at the nozzle outlet, needed to obtain the momentum flux per unit length of jet,  $J$ , were made using a  $5 \mu\text{m}$  single hot wire probe and a DISA 55D01 constant temperature anemometer. The unknown variation of static pressure across the jet precluded the use of a total head tube to measure mean velocity. A pitot-static probe was not used because  $t$  was too small.

All velocity and lift measurements were made on the centre-line of the nozzle span,  $z=0$ . To simulate the conditions in an actual floatation oven, the wind tunnel fan speed was held constant, so that the momentum flux,  $J$ , monotonically increased with  $h$  in all cases except for the unblocked flow in NB1. Full details of the experimental techniques are given in Davies (1984).

## 3 ASPECT RATIO EFFECTS

Figure 2 shows  $A_e$ , the experimental coefficient of ground effect, for both nozzle boxes for a jet exit velocity of around 25 m/s. Figure 2 shows the measurements taken with and without end plates. We begin by discussing the former. The distribution of "infinite"  $A_e$  differs between NB1 and NB2. Possible causes of the discrepancy are experimental error (DW estimated the accuracy of  $A_e$  to be about 14% suggesting good agreement with the basic theory), slight changes in nozzle geometry, differences between wind tunnels and differences in measurement techniques. There is no obvious single cause; it is suggested that a combination of small errors due to the above causes has occurred. The remaining possibility is that the aspect ratio for NB1 is so small that blocking the ends cannot reproduce an "infinite" aspect ratio flow. However, the many checks demonstrated (not shown) good two-dimensionality of the blocked flow in NB1, so we regard this possibility as unlikely.

TABLE 1

NOZZLE DIMENSIONS

| Nozzle | t(mm) | b(mm) | w(mm) | AR   |
|--------|-------|-------|-------|------|
| NB1    | 5     | 75    | 375   | 5    |
| NB2    | 5     | 75    | 1000  | 13.3 |
| Actual | 6.7   | 100   | 1450  | 14.5 |

The results for each nozzle box are self-consistent in that  $A_e$  for no end plates is always less than  $A_e$  for end plates, as blockage of flow improves the conversion of momentum into force. In the rest of this paper we will use the term "aspect ratio effects" to mean the difference between the blocked flow (with end plates) and unblocked flow (without end plates) results for each nozzle box. Figure 2 suggests that aspect ratio effects are significant for NB1 but are not so for NB2.

### 3.1 Further Effects at High Aspect Ratio

Figure 2 suggests that the unblocked flow in NB2 was close to two-dimensional. However, spanwise checks of plate surface total head, measured at  $x/b=2$ , shown in Figure 3, demonstrate a significant lack of two-dimensionality. These results are consistent with surface pressure measurements taken along the z-axis, which are not presented. The two-dimensionality of flow initially decreases as  $h/t$  increases, although the uniformity at  $h/t = 15$  is better than that at  $h/t = 8$ . The results in the case of no end plates are not symmetric about the nozzle span centre-line. This supports the suggestion of wind tunnel and/or nozzle geometry effects causing differences in the  $A_e$  results of NB1 and NB2.

The lack of two-dimensionality in an actual floatation oven is not necessarily significant if the spanwise variations in the upper and lower nozzles are similar and the variations are roughly symmetric about  $z=0$ .

### 3.2 Further Effects at Low Aspect Ratio

Figure 4 shows the lift characteristics of NB1, rather than  $A_e$ , with and without end plates. At small  $h/t$ , and then again at large  $h/t$ , the lift characteristics for both cases are similar. However, there is a peculiar dip, over the range  $4 < h/t < 12$ , in the lift characteristic for the system with no end plates which is related to the dependence of  $J$  on  $h$  as explained earlier. This dip is independent of Reynolds number and would produce an instability in the opposing nozzle system in an actual floatation oven.

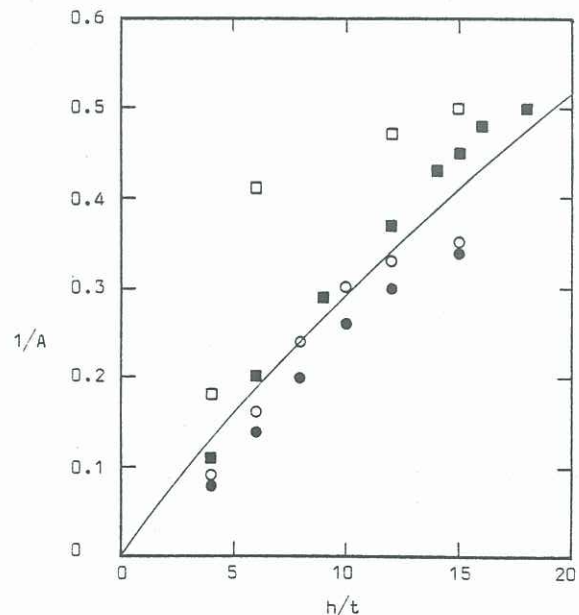


Figure 2 Experimental and theoretical coefficients of ground effect.  $\square$ , NB1;  $\circ$ , NB2. Open symbols are unblocked flow, solid symbols are blocked flow. Solid line is from equation (2).

The dip occurs at a line of symmetry where z-dependent effects should be minimal. Furthermore, the aspect ratio of the individual jets,  $w/t$ , is significantly higher than that known to produce reasonably two-dimensional flow in single jets. Thus it is likely that the dip is associated with some form of interaction between the jets. Note that if the jets remained thin and followed the constant trajectory of  $\Theta=30^\circ$  they would meet at  $h/t=8.7$ . The most likely explanation is that the jets are interacting via their pressure fields. Presumably, the escape of air cushion fluid (Figure 1) from between the jets and out the edges (in the z-direction), will bring the jets closer together in the mean, although some periodic bodily and coherent movement of the two jets is likely. Attaching end plates to the nozzle edges prevents this mechanism from working by stopping the air cushion fluid from escaping. Consequently, the two jets are forced further apart than in the case of no end plates, so that no interaction occurs. This conjecture is supported by the finding that the point of maximum plate pressure moves outward when end plates are installed, suggesting that the mean reattachment point also moves outward. These results are not shown.

#### 4 CAUSES OF ASPECT RATIO EFFECTS

A detailed investigation into the dynamics of the interacting jets was not possible with the equipment available. However, to test the hypothesis of jet interaction, some simple, further experiments were undertaken.

Any free shear layer that eventually attaches to a solid surface can experience "feedback" effects which, contrary to the boundary layer approximation, can propagate upstream and significantly modify the flow structure (Rockwell & Naudascher, (1979)).

This feedback usually modifies the power spectra of the fluctuating velocities, at least at low Reynolds number, leading to pronounced peaks at the characteristic frequency or frequencies. Spectra obtained in the fully turbulent part of the flow from NB1 did not display any unusual features so we measured the spectra in the transition region just downstream of the jet exit for  $4 < h/t < 12$ . Figure 5 shows the results at  $h/t=8$  for the blocked and unblocked flows. The differences are minimal, suggesting that no significant feedback occurred in the unblocked flow case. Thus, the differences shown in Figure 4 were caused by the effect of blocking or unblocking on the fully turbulent part of the flow only.

The interaction of the jets via the expulsion of air cushion fluid would have to occur coherently over a large spanwise distance to be effective, as any small scale (in the z-direction) random oscillations of the jets would tend to produce little net effect. In an attempt to destroy any spanwise coherence in the jets, "vortex generators", consisting of lengths of string, were placed across the two jet exits, parallel to the x-axis and 15 mm apart. This spacing was large compared to the jet thickness and hence larger than the biggest eddies in the jet, if they were wholly three-dimensional. Figure 4 shows that the vortex generators increased the lift by around 30% for the unblocked flow case, bringing the results closer to the blocked flow values (with no vortex generators), whereas the decrease in the lift for the blocked flow case was much smaller. Thus, the results are consistent with the hypothesis that the fully turbulent part of the jets interact in the unblocked flow.

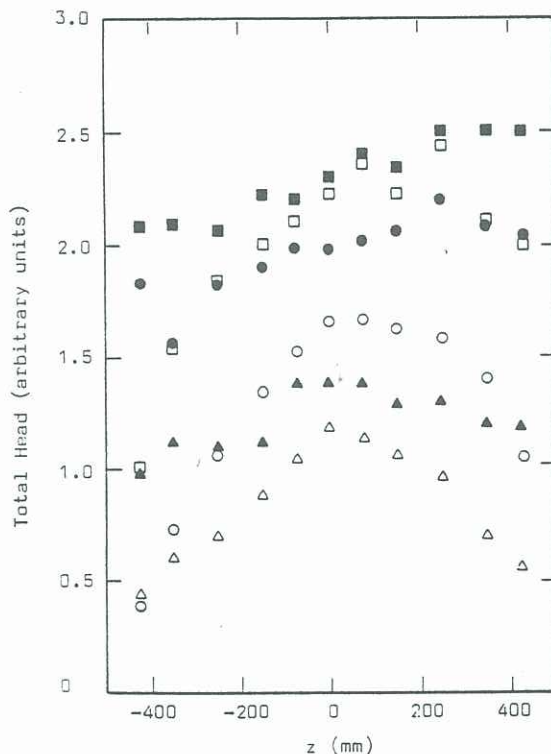


Figure 3 Spanwise distribution of surface total head at  $x/b = 2$  for NB2.  $\square$ ,  $h/t = 2$ ;  $\circ$ ,  $h/t = 8$ ;  $\triangle$ ,  $h/t = 15$ . Open symbols are unblocked flow, solid symbols are blocked flow.

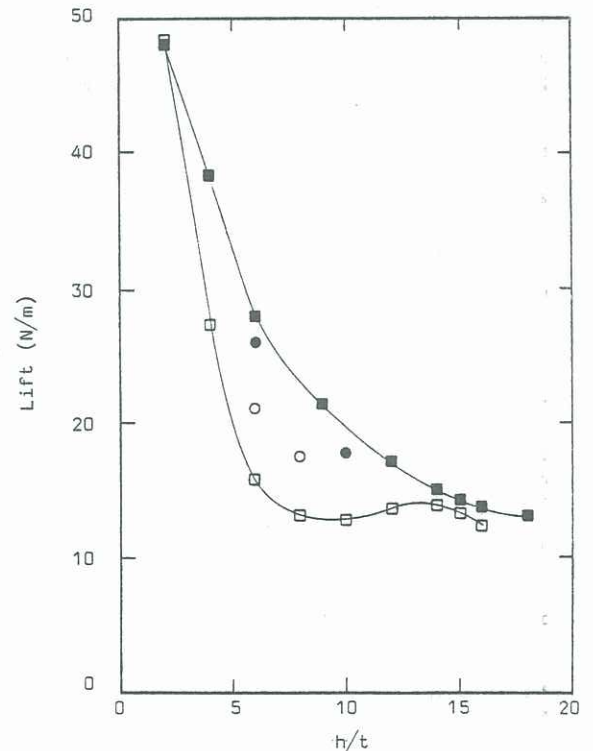


Figure 4 Lift characteristics of NB1.  $\square$ , unblocked flow;  $\blacksquare$ , blocked flow. With vortex generators, as described in text:  $\circ$ , unblocked flow;  $\bullet$ , blocked flow.

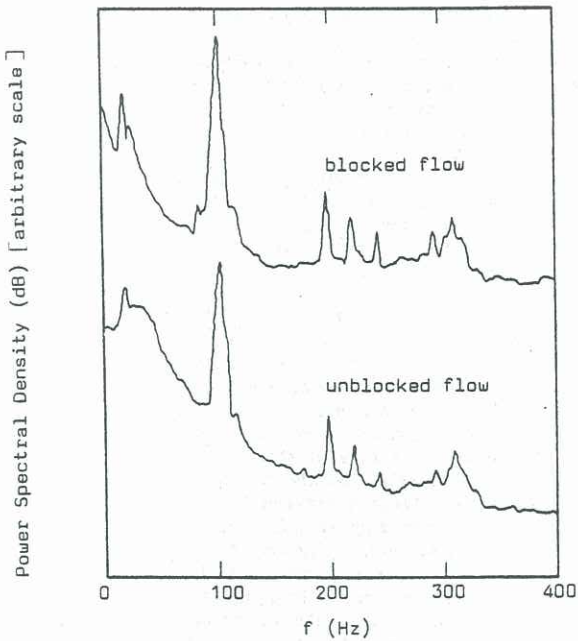


Figure 5 Transition spectra of velocity fluctuations at  $h/t = 8$  for NB1.

## 5 CONCLUSIONS

The results show that the simple theory works reasonably well along the centre-line of the model (NB2) with an aspect ratio comparable to the actual nozzles in a floatation oven, whether or not end plates were used to improve the two-dimensionality. The major aspect ratio effects

in NB2 were the significant spanwise variations in the lift. These are unlikely to be important if there is similarity in the spanwise characteristics of the upper and lower nozzles in a floatation oven and the variations are roughly symmetric about  $z=0$ . Therefore, the present results suggest that the simple theory, leading to equation (2), is a reasonable description of the flow in an actual floatation nozzle. Furthermore, the experiments could be used to obtain an empirical modification to equation (2) for the actual nozzles in a floatation oven.

The significantly lower aspect ratio of NB1 produced an unexpected local minimum in the lift as a function of height. It appears that this behaviour is associated with the interaction of the fully turbulent part of the inclined jets over the range  $4 < h/t < 12$ . This hypothesis is consistent with the measured spectra and the results of modifying the flow using "vortex generators". It is remarkable that the attachment of strings across the jets can increase the lift by 30%.

## 6 ACKNOWLEDGEMENT

The authors are grateful to John Lysaght (Australia) Limited for supporting this work. The automated data collection system was designed and built by Mr Ian Miller, who also provided the software.

## 7 REFERENCES

- DAVIES, M.J. and WOOD, D.H. (1983) The Basic Aerodynamics of Floatation. *ASME J. Fluids Eng.*, **105**, (to appear).
- DAVIES, M.J. (1984) M.E. Thesis. In preparation.
- JAUMOTTE, A. and KIEDRZYNSKI, A. (1964) Theory and Experiments on Air Cushion Vehicles at Zero Speed. *Hovering Craft and Hydrofoil*, **4**, 4-25.
- ROCKWELL, D. and NAUDASCHER, E. (1979) Self-Sustained Oscillations of Impinging Free Shear Layers. *Ann. Rev. Fluid Mech.*, **11**, 67-94.